THE ARCHIVE OF MECHANICAL ENGINEERING

Vol. XLVIII 2001 Number 1

Key words: *stiffener, buckling, plate, beam, thin-walled structure, interactive buckling, load carrying capacity, design code, ultimate load, imperfection.*

ANDRZEJ TETER[*)], *ZBIGNIEW KOLAKOWSKI*[**)]

COMPARISON OF THE THEORETICAL LOAD CARRYING CAPACITY WITH THE EXPERIMENTAL DATA FOR SOME THIN-WALLED PLATES AND BEAMS WITH INTERMEDIATE STIFFENERS

In the present paper, an analysis of lower bound estimation of the load carrying capacity of structures with intermediate stiffeners is undertaken. Thin-walled structures with intermediate stiffeners in the elastic range, being under axial compression and a bending moment, are examined on the basis of the Byskov and Hutchinson's method [4] and the co-operation between all the walls of the considered structures is shown. The structures are assumed to be simply supported at the ends. The study is based on the numerical method of the transition matrix using Godunov's orthogonalization [2]. Instead of the finite strip method, the exact transition matrix method is used in this case. In the presented method for lower bound estimation of the load carrying capacity of structures, it is postulated that the reduced local critical load should be determined taking into account the global pre-critical bending within the first order non-linear approximation to the theory of the interactive buckling of the structure. The results are compared to those obtained from the design code and the data reported by other authors.

The present paper is a continuation of papers [9], [11], [19], where the interactive buckling of thin-walled beam-columns with central intermediate stiffeners in the first and the second order approximation was considered.

The most important advantage of this method is that it enables us to describe a complete range of behaviour of thin-walled structures from all global (flexural, flexural-torsional, lateral, distortional and their combinations) to local stability. In the solution obtained, the effects of interaction of modes, the transformation of buckling modes with an increase in load, the shear lag phenomenon and also the effect of cross-sectional distortions are included.

[*)] *Department of Applied Mechanics, Technical University of Lublin; ul. Nadbystrzycka 36, 20-618 Lublin, Poland; E-mail: teter@archimedes.pol.lublin.pl*

[**)] *Department of Strength of Materials and Structures, Technical University of Łódź; ul. B. Stefanowskiego 1/15, 90-924 Łódź, Poland; E-mail: kola@oriol.p.lodz.pl*

NOTATION

A, A_e — cross-section area and the effective part of the cross-section area A, respectively,

a_o, a_r, a_{ijkr}, b_{jklr} — coefficients in non-linear equilibrium equations (4) [4], [15],

b, b_e — plate width and the effective part of the plate, respectively,

b_i — width of the i-th wall of the structure,

E — Young's modulus,

f_d — design strength (for this application $f_d=R_e$),

i — cross-section radius of gyration,

I_{adeq} — minimum allowable moment of inertia (adequate moment) with respect to the axis going through the middle surface of the element to be stiffened – BS 5950 Part 5,

I_S — actual moment of inertia of the full stiffener with respect to the axis going through the middle surface of the element to be stiffened – BS 5950 Part 5,

J — number of the interacting mode,

j — number of the mode,

L — length of the structure,

l_o — calculational length of the beam,

M_{cr}, $\overline{M}_{cr}$ — theoretical and experimental critical moment, respectively,

M_E, $\overline{M}_E$ — theoretical and experimental limit moment, respectively,

$\overline{M}_{EF}$ — limit moment according to BS 5950 Part 5,

M_{ix}, M_{iy}, M_{ixy} — bending moment resultants for the i-th wall,

M_u — ultimate moment capacity,

M_{pl} — yield moment,

$\overline{\mathbf{N}}$ — force field,

N_{ix}, N_{iy}, N_{ixy} — in-plane force resultants for the i-th wall,

P_{cr}, $\overline{P}_{cr}$ — theoretical and experimental critical force, respectively,

$\overline{P}_{EF}$ — load carrying capacity according to BS 5950 Part 5,

P_1 — yield load,

P_R — reduced critical force,

P_U, $\overline{P}_E$ — theoretical and experimental load carrying capacity, respectively,

P_{UR} — reduced load carrying capacity,

P_u — ultimate load capacity,

R_e — conventional yield limit,

s, $\overline{s}$ — slenderness and relative slenderness, respectively,

t — thickness of the plate,

t_i — thickness of the i-th wall of the structure,

u_i, v_i, w_i — displacement components of the middle surface of the i-th wall,
$\bar{U}$ — displacement field,
Z — the section modulus of the cross section,
Z_e — effective section modulus for the whole section,
η_K — coefficient of the reduced rigidity corresponding to the K-th uncoupled local buckling mode,
$\kappa_{ix}, \kappa_{iy}, \kappa_{ixy}$ — curvature modifications and torsions of the middle surface of the i-th wall,
δ — ratio of the stiffener cross-section area to the web wall cross-section area,
$\varepsilon_{ix}, \varepsilon_{iy}, \varepsilon_{ixy}$ — strain tensor components of the middle surface of the i-th wall,
ζ_j — amplitude buckling mode number j,
ζ_j^* — imperfection amplitude corresponding to ζ_j,
λ — scalar load parameter,
λ_j — value of λ at the bifurcation mode number j,
λ_s — maximum value of λ for the imperfect structure,
λ_R — reduced critical value of the local buckling mode,
μ — coefficient of fixing,
ν — Poisson's ratio,
$\sigma_{cr}^* = \sigma_{cr} 10^3 / E$ — dimensionless critical stress of the j-th mode,
σ_c — compressive stress,
σ_{cr} — critical stress of the element,
σ_u — stress at the ultimate load,
φ_p, φ — local and global instability coefficient, respectively.

1. Introduction

Analysis of buckling of conservative systems belongs to the main problems that have been studied in mechanical sciences for a number of years. The comprehensive reviews of the literature concerning buckling can by found in [13], [15].

Local buckling is the major feature to be taken into account in the design of thin-walled sections. Thin-walled structures, especially plates, columns and beams, may have many buckling modes and are able to sustain load after local buckling. The local buckles cause reduction in the stiffness of a section and, consequently, lower the load carrying capacity relative to a non-locally buckled section. The determination of their load carrying capacity requires consideration of the modal interaction of buckling modes and imperfections in the non-linear

analysis of stability. The problem of the interaction of the global mode with the local ones is of great significance. The concept of interactive buckling involves the general asymptotic non-linear theory of stability. The theory is based on asymptotic expansions of the post-buckling path and is capable of considering simultaneous or nearly simultaneous buckling modes [4], [15].

The introduction of central intermediate stiffeners increases the flexural rigidity of plate elements and, consequently, also the local critical stress values. The global critical stress values for the analysed type of intermediate stiffeners remain virtually unchanged because of small variations in the moment of inertia of the cross-section.

Structures reinforced with intermediate stiffeners may show two local minima for two different local buckling modes. The first minimum refers to the smaller number of half-waves (local distortional mode) and the second one – to the greater number of half-waves (local symmetric mode and local antisymmetric mode) as compared with the structure without reinforcement. In particular cases, the values of these minima for local buckling modes can be almost equal.

Special attention should be paid to the fact that critical stress values referring to the second minimum are nearly equal for both local modes. The theory presented here enables us to carry out an analysis of all buckling modes for intermediate stiffeners of different shapes and flexural rigidities. This can help in their rational designing (for a more detailed analysis, see [9], [11], [19]).

In this paper, the solution has been obtained by Koiter's asymptotic method in the second order approximation. The determined post-buckling coefficients allow one to find the flexural rigidity after local buckling without using hypotheses on the effective width of plates under eccentric compression. Simple analytical dependencies between the above mentioned coefficients and the characteristics of the post-buckling equilibrium path are used [16].

In many scientific centres, intensive theoretical and experimental investigations devoted to buckling of structures with boundary reinforcements, intermediate stiffeners and the so-called mesostructures and aimed at a comparison of these investigation results with standards in force are conducted. Main problems, as far as theoretical issues are concerned, consist in a proper description of all possible global and local buckling modes, as well as in a presentation of analytical relations in a coherent form that is convenient for application in standards. The authors of the present paper do not know any works by other authors in which all buckling modes of thin-walled structures with intermediate stiffeners have been described correctly. This paper belongs to a series of publications by the authors aimed at this purpose.

2. Structural problem

The long thin-walled prismatic structures of the length L, composed of plane, rectangular plate segments interconnected along longitudinal edges, simply

supported at both ends, are considered. A plate model is adopted for the structures with intermediate stiffeners. For the i-th plate component, precise geometrical relationships are assumed in order to allow for the consideration of both out-of-plane and in-plane bending of each plate [11]:

$$\begin{aligned} \varepsilon_{ix} &= u_{i.x} + \tfrac{1}{2}(w_{i.x}^2 + v_{i.x}^2), \\ \varepsilon_{iy} &= v_{i.y} + \tfrac{1}{2}(w_{i.y}^2 + u_{i.y}^2), \\ 2\varepsilon_{ixy} &= \gamma_{ixy} = u_{i.y} + v_{i.x} + w_{i.x} w_{i.y}, \\ \kappa_{ix} &= -w_{i.xx}, \quad \kappa_{iy} = -w_{i.yy}, \quad \kappa_{ixy} = -w_{i.xy}. \end{aligned} \tag{1}$$

The differential equilibrium equations resulting from the virtual work principle and corresponding to expressions (1) for the i-th plate can be written as follows:

$$\begin{aligned} N_{ix.x} + N_{ixy.y} + \left(N_{iy} u_{i.y}\right)_{.y} &= 0, \\ N_{ixy.x} + N_{iy.y} + \left(N_{ix} v_{i.x}\right)_{.x} &= 0, \\ \left(N_{ix} w_{i.x}\right)_{.x} + \left(N_{iy} w_{i.y}\right)_{.y} + \left(N_{ixy} w_{i.x}\right)_{.y} + \left(N_{ixy} w_{i.y}\right)_{.x} + M_{ix.xx} + M_{iy.yy} + 2M_{ixy.xy} &= 0. \end{aligned} \tag{2}$$

The solution of these equations for each plate should satisfy kinematic and static continuity conditions at the junctions of adjacent plates and the boundary conditions referring to the free support of the structure at its both ends, i.e. x=0 and x=L.

The non-linear problem is solved by the Byskov and Hutchinson's asymptotic method [4]. The displacement fields, $\bar{\mathbf{U}}$, and the sectional force fields, $\bar{\mathbf{N}}$, are expanded in power series in the buckling mode amplitudes, ζ_j (ζ_j is the amplitude of the j-th buckling mode divided by the thickness of the first component plate, t_1):

$$\begin{aligned} \bar{\mathbf{U}} &= \lambda \bar{U}_i^{(0)} + \zeta_j \bar{U}_i^{(j)} + \zeta_j \zeta_k \bar{U}_i^{(jk)} + \ldots \\ \bar{\mathbf{N}} &= \lambda \bar{N}_i^{(0)} + \zeta_j \bar{N}_i^{(j)} + \zeta_j \zeta_k \bar{N}_i^{(jk)} + \ldots \end{aligned} \tag{3}$$

where the pre-buckling fields are $\bar{U}_i^{(0)}, \bar{N}_i^{(0)}$, the buckling mode fields are $\bar{U}_i^{(j)}, \bar{N}_i^{(j)}$ and the post-buckling fields — $\bar{U}_i^{(jk)}, \bar{N}_i^{(jk)}$. The range of indices is [1, J], where J is the number of interacting modes.

By substituting expansion (3) into equations of equilibrium (2), the junction conditions and the boundary conditions, the boundary value problems of the zero, first and second order can be obtained. The zero approximation describes the pre-buckling state, while the first approximation, that is the linear problem of stability, enables us to determine critical loads of the global and local value and their buckling modes. The second order boundary problem describes the post-buckling equilibrium path. For a more detailed analysis, see [11].

At the point where the load parameter λ reaches its maximum value λ_s (secondary bifurcation or limit point) for the imperfect structure with regard to the imperfection of the buckling mode with the amplitude ζ_r^*, the Jacobian of the non-linear system of equations [4], [11], [15]:

$$a_r\left(1-\frac{\lambda}{\lambda_r}\right)\zeta_r + a_{jkr}\zeta_j\zeta_k + b_{jklr}\zeta_j\zeta_k\zeta_l + \ldots = a_r\frac{\lambda}{\lambda_r}\zeta_r^* \quad \text{at } r=1,2,\ldots..J \tag{4}$$

is equal to zero.

The index "r" is: 1 — for the global bulking mode; 2...J — for the local buckling modes.

The corresponding expression for the total elastic potential energy of the structures has the following form:

$$\Pi = -a_o\lambda^2/2 + a_r(1-\lambda/\lambda_r)\zeta_r^2/2 + a_{jkr}\zeta_j\zeta_k\zeta_r/3 + b_{jklr}\zeta_j\zeta_k\zeta_l\zeta_r/4 - a_r\zeta_r\zeta_r^*\lambda/\lambda_r \tag{5}$$

where: λ — load parameter, λ_r — critical value of λ, $\Pi_o = a_o\lambda^2/2$ — energy of the pre-buckling state.

Expressions for a_o, a_r, a_{jkr}, b_{jklr} are calculated by known formulae [4], [11], [15], [16]. The formulae for the postbuckling coefficients a_{jkr} depend only on the buckling modes, whereas the coefficients b_{rrrr} also depend on the second order field.

Consideration of displacements and load components in the middle surface of the walls within the first order approximation, as well as more precise geometrical relationships made it possible to analyse the shear-lag phenomenon, the distortions of cross-sections and all possible buckling modes including a mixed buckling mode (e.g. flexural-distorsional or local-distorsional one — for a more detailed analysis, see [5], [7], [11], [12], [14]).

The calculations have confirmed that in the case when the value of the global critical load exceeds the value of the local critical load, it is possible to reach the limit load capacity higher than the minimum value of the local critical load for a moderately low value of the imperfection.

Taking into account the second order approximation enables us to determine the limit load capacity of the structure in an elastic range. An assumption of one of the "engineering" hypotheses of the load carrying capacity allows for determination of the limit load for an elastic-plastic range [10], [16].

The relation between the post-buckling and unbending pre-buckling stiffness of imperfect structures defines a coefficient of the reduced rigidity corresponding to the K-th uncoupled local buckling, i.e. the single-mode local buckling [11], [16]:

$$\eta_K = \left[1+\frac{a_K\zeta_K\lambda_K}{a_o\lambda}\left(0.5\zeta_K+\zeta_K^*\right)\right]^{-1} \quad \text{at } K = 2,\ldots J \tag{6}$$

In a special case of ideal structures ($\zeta_K^* = 0$) and of the symmetrical characteristics relative of the deflections for the uncoupled local buckling mode ($a_{KKK} = 0$):

$$\bar{\eta}_K = \lim_{\lambda \to \infty} \eta_K = \left[1 + \frac{a_K^2}{2a_0 b_{KKKK}} \right]^{-1} \tag{7}$$

In the presented method for lower bound estimation of the load carrying capacity, it is postulated that the reduced local critical load λ_R should be determined taking into account the global pre-critical bending ($\zeta_1^* \neq 0$) within the first order non-linear approximation to the theory of the interactive buckling of the structure. In order to find lower bound estimation of the load carrying capacity of thin-walled structures, the following assumptions, identical as in paper [17], have been made:

- an interaction of only two modes of the global and local buckling within the first order approximation has been taken into account, i.e. J=2;
- the local buckling precedes the global buckling, i.e. $\lambda_1 > \lambda_2$ ($\sigma_1^* < \sigma_2^*$);
- local imperfections are absent, i.e. $\zeta_2^* = 0$.

If we take into account the above-mentioned assumptions, Eq. (4) leads to the following set of algebraic equations of equilibrium:

$$\begin{aligned} a_1 (1 - \lambda/\lambda_1)\zeta_1 + a_{122}\zeta_2^2 &= a_1 \zeta_1^* \lambda/\lambda_1 \\ a_2 (1 - \lambda/\lambda_2)\zeta_2 + 2a_{122}\zeta_1\zeta_2 &= 0 \end{aligned} \tag{8}$$

All coefficients with j, k, r > 1 are equal to zero and non-zero coefficients are only those that have one index equal to 1 and an even sum of (j+k). If we introduce the following notation:

$$\vartheta = \left(\frac{\lambda}{\lambda_2} - 1 \right) \frac{1}{\zeta_1}, \tag{9}$$

the second equation (8B) can be written in the form of an eigenvalue problem:

$$\left(2\frac{a_{122}}{a_2} - \vartheta \right) \zeta_2 = 0. \tag{10}$$

In the pre-buckling state, the single solution to Eq. (10) is a trivial solution $\zeta_2 = 0$ and only the overall deflection develops according to Eq. (8A):

$$\zeta_1 = \zeta_1^* \frac{\lambda}{\lambda_1 - \lambda}. \tag{11}$$

The coupled (interactive) buckling with simultaneous overall and local deflections becomes possible when there appears a non-zero solution $\zeta_2 \neq 0$ to the set of Eqs. (10). Note that the sign of $\vartheta = 2a_{122}/a_2$ determines the direction of the overall deflection according to the condition $\vartheta\zeta_1 < 0$.

The eigenvector from Eq. (10) has been determined with accuracy up to the constant C and it has been normalised with the condition $[(\zeta_2^0)^2]^{1/2} = 1$. Hence, eq. (8A) can be written in the form:

$$C^2 = \frac{a_1}{a_{122}\left(\zeta_2^0\right)^2}\left[\zeta_1^* \frac{\lambda}{\lambda_1} + \left(1-\frac{\lambda}{\lambda_1}\right)\left(1-\frac{\lambda}{\lambda_2}\right)\frac{1}{\vartheta}\right]. \tag{12}$$

As the initial post-buckling path for the first order approximation always falls, the maximal value $\lambda=\lambda_R$ corresponds to the value C=0 (the point of intersection of the pre-buckling path (11) and the initial post-buckling path (9)). Then, Eq. (12) assumes the following form:

$$\left[\zeta_1^* \frac{\lambda_R}{\lambda_1} + \left(1-\frac{\lambda_R}{\lambda_1}\right)\left(1-\frac{\lambda_R}{\lambda_2}\right)\frac{1}{\vartheta}\right] = 0. \tag{13}$$

The maximum load value λ_R determined from Eq. (13) is smaller than the critical value of the local buckling λ_2. The load λ_R can be interpreted as an effect of the load corresponding to the global buckling ($\zeta_1^* \neq 0, \zeta_1 \neq 0$) on the critical value of the local load ($\zeta_{21} \neq 0$). Thus, the critical load corresponding to λ_R can be called the reduced critical load value of the local buckling. For the load $\lambda_R<\lambda<\lambda_2$, the coefficient of reduced rigidity (specified by relation (6)) is equal to $\eta_2=\eta_K=1$. Hence, it is postulated that λ_R should substitute $\lambda_2=\lambda_K$ in eqs. (6) and (7). A further procedure to determine lower bound estimation of the load carrying capacity is analogous as in [10], [16]. This load carrying capacity can be determined on the basis of an appropriate strength (effort) criterion. The following criterion for stiffened constructions is assumed: "plastic stresses are reached in the elements for the limit load higher than the critical load". More detailed analysis see p. 4. of the present paper.

3. Design code recommendations

3.1. Calculation according to the Winter's formula

The Winter's formula is commonly used in design procedures to determine an estimate of the ultimate load carrying capacity of plates under compression (e.g. [1], [6]). In its usual form it is expressed as:

$$\frac{b_e}{b} = 1 \qquad s \le 0{,}673$$

$$\frac{b_e}{b} = \frac{1}{s^2}(s-0{,}22) \qquad s > 0{,}673 \tag{14}$$

where: $s = \sqrt{\frac{R_e}{\sigma_{cr}}}$ - relative slenderness.

The reduction made on the basis of the local mode is based on the Winter's rule, which is used instead of one plate to the whole cross-section. In this method, the supporting influence of other plates is taken into account, and the whole cross-section of the profile is reduced. This is equivalent to:

$$\frac{A_e}{A}=\sqrt{\frac{\sigma_{cr}}{R_e}}\left(1-0,22\sqrt{\frac{\sigma_{cr}}{R_e}}\right)=\frac{\sigma_u}{R_e} \tag{15}$$

The axial ultimate load capacity is expressed as:

$$P_u=R_eA_e \tag{16}$$

If a similar approach is applied to members under flexure, then, by a direct analogy with (15), the effective section modulus (Z_e) is calculated as:

$$\frac{Z_e}{Z}=\sqrt{\frac{\sigma_{cr}}{R_e}}\left(1-0,22\sqrt{\frac{\sigma_{cr}}{R_e}}\right) \tag{17}$$

leading thus to the ultimate moment capacity:

$$M_u=R_eZ_e \tag{18}$$

In (17), the effective section modulus Z_e does not represent effective widths of individual elements.

In the proposed method, the design yield stress depends on the yield stress reduced by the global mode. The aim of this is to avoid decreasing the effective yield stress caused by high material strength, if it is not utilized because of the global mode.

3.2. Calculation according to the Polish Code PN-90/B-03200 [18]

In the post-buckling state for each wall that forms the cross-section under analysis, the effective width $b_e=\varphi_{pe}b$ is determined. The value of the instability coefficient φ_p and φ_{pe} is determined from the table [18] for the calculated wall slenderness:

$$\bar{s}_p=\frac{b}{t}\cdot\frac{K}{56}\sqrt{\frac{f_d}{215}} \tag{19}$$

where K — wall support and load coefficient.

In the critical state for the wall under axial compression we have:

$$\frac{\sigma_c}{\varphi_p f_d}\le 1 \tag{20}$$

where: σ_c — highest compressive stress in the wall under consideration.

For the obtained effective widths, the effective area $A_e<A$ is determined in the case of axial compression, whereas in the case of pure bending — the effective factor of strength $W_e<W$. In the case of eccentric compression, the area A_e determined as under uniform compression can be assumed, and the factor W_e — determined as under pure bending conditions. Additionally, an increment in the loading moment resulting from a change in the position of the centroid of the effective cross-section should be accounted for.

The value of the reduction coefficient of the cross-section calculational load carrying capacity ψ is equal to:

a) critical state: $\psi=\varphi_p$;

b) post-critical state: $\psi=\psi_e$;

For axial compression: $\Psi_e = \frac{A_e}{A}$, whereas for pure bending: $\Psi_e = \frac{W_e}{W}$.

In the case of intermediate stiffeners, it should be assumed that their moment of inertia with respect to the web symmetry axis equals: $I_s \geq kbt^3$ (stiffness condition), where the coefficient $k = 3\frac{L}{b}\sqrt{\frac{L}{b}\delta}$, but $k \geq 0,7\frac{L}{b}\sqrt{\frac{L}{b}}$ and L>b.

In the post-buckling state, additionally the stiffener load carrying capacity should be checked. The stiffener should be treated as a freely supported beam loaded with the force whose value is equal to 2% of the compressive force in the wall.

The total effective area is: $A_e = A_z + \sum b_e t$, where A_z – stiffener area.

The beam slenderness should satisfy the condition s<250.

The compression capacity is:

$$N_{RC} = \Psi A f_d \tag{21}$$

if the yield phenomenon precedes the stability loss, then the coefficient $\psi=1$.

The beam relative slenderness under buckling is equal to: $\bar{s} = \frac{s}{s_p}$, where the comparative slenderness is $s_p = 84\sqrt{\frac{215}{f_d}}$, and the beam slenderness is $s = \frac{\mu l_o}{i}$.

For the determined beam relative slenderness $\bar{s}$, the coefficient φ is read from the table [18].

The design buckling resistance:

$$N = \varphi N_{RC}. \tag{22}$$

In the case of pure bending, the limit moment is equal to:

$$M_R = \Psi W f_d. \tag{23}$$

For the given value of the relative slenderness under lateral buckling $\bar{s}_L = 1,15\sqrt{\frac{M_R}{M_{cr}}}$, the lateral buckling coefficient φ_L is taken from the table ([18]), and then the calculational moment is determined:

$$M = \varphi_L M_R. \tag{24}$$

3.3. Calculation according to BS 5950 Part 5 [3]

The effects of local bucking should be taken into account in determination of the design strength and stiffness of cold-formed members. This may be accomplished using effective cross-sectional properties, which are calculated on the basis of the widths of individual elements. The ratio of the effective width b_e

to the full width b of an element under compression may be determined from the following expression:

for $(b/h)<60$ and $(\sigma_C/\sigma_{cr})<0,123$ - $(b_e/b)=1$,

for $(b/h)<60$ and $(\sigma_C/\sigma_{cr})>0,123$ - $(b_e/b)=[1+14(\sqrt{\sigma_c/\sigma_{cr}}-0,35)^4]^{-0,2}$ (25)

where the width to thickness ratio exceeds 60, the effective design width of the sub-element should be reduced according to the following formula: $(b_{er}/t)=b_e/b-0,1(b/t-60)$.

To compute the effective properties of a member having compression sub-elements subject to the above reductions in the effective width, the area of stiffeners, A_{st}, should be considered to be reduced to the effective area, A_{eff}, as follows:

for $(b/h)<60$ to $A_{eff}=A_{st}$,

for $60<(b/h)<90$ – $A_{eff}=A_{st}\left[3-2\frac{b_{er}}{b}-\frac{1}{30}\left(1-\frac{b_{er}}{b}\right)\frac{b}{h}\right]$, (26)

for $(b/h)>90$ - $A_{eff}=A_{st}(b_{er}/b)$.

In the above expressions A_{st} and A_{eff} refer only to the area of the stiffener alone, irrespective of any portion of adjacent elements.

The centroid of the stiffener should be considered to be located at the centroid of the full area of the stiffener, and the moment of inertia of the stiffener about its own centroidal axis should be taken as that of the full section of the stiffener.

The axial ultimate load capacity is expressed as follows:

$$P_c=R_eA_e \tag{27}$$

This equation is only suitable for columns with very small values of the slenderness ratio (i.e. the ratio of the column length to the cross-section radius of gyration, $L/r < 20$), sometimes referred to as 'stub columns'. At low L/r ratios, P_c tends to the squash load (P_{cs}) value, and to evaluate the interaction of buckling and yield for larger L/r ratios, the Perry-Robertson approach provided in the design code is used.

The buckling resistance is as follows:

$$P_c=0,5\left\{[P_{cs}+(1+\eta)P_E]-\sqrt{[P_{cs}+(1+\eta)P_E]^2-4P_{cs}P_E}\right\} \tag{28}$$

where: P_{cs} - squash load ($P_{cs}=P_c$ for short columns); P_E – elastic flexural buckling load; η - Perry coefficient [3].

If a similar approach is applied to members under flexure, the effective section modulus (Z_e) is calculated [3]. The ultimate moment capacity is expressed as:

$$M_u=R_eZ_e. \tag{29}$$

4. Comparison of the theoretical load carrying capacity with the experimental data and design methods

In the general case, the load carrying capacity can be determined on the basis of the appropriate strength (effort) criterion. At this point of the present work, the following criterion of the limit load carrying capacity for stiffened constructions is assumed: "plastic stresses are reached in the elements for the limit load higher than the critical load".

4.1. Thin-walled plates with central intermediate stiffeners

Compressed rectangular plates with central intermediate V-stiffeners have been analysed in detail. The dimensions of the plates under analysis, with the length L and freely supported along the whole perimeter (Fig. 1), are the same as in [8].

A comparison of the results obtained on the basis of the presented theory with the experimental results shown in [8] has been made.

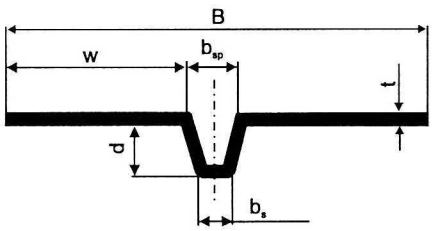

Fig. 1. Cross-section of the plate with a central intermediate stiffener

In Table 1, the dimensions of the plates under analysis and the mean values of the yield limit R_e are collected. The following values of the Young's modulus and the Poisson's ratio have been assumed: E=205 GPa and v=0,3, respectively.

The results calculated by different methods are gathered in Table 2. The theoretical P_R and experimental values P_{UR} of the limit loads corresponding to λ_R for $\zeta_1^* = L/1000t$ are compared to the results calculated in two other manners. The codes used were the British code BS 5950 Part 5 [3] and the method based on the Winter's formula. In Table 1, the results of calculations carried out according to the Polish code PN-90/B-03200 have not been included, as the plates under analysis do not fulfil the requirements imposed by this code as regards slenderness that has to be higher than 250.

Table 1.

Dimensions of the plates with a central intermediate stiffener [8]

No.	Spec. no.	R_e [MPa]	L [mm]	w [mm]	b_s [mm]	b_{sp} [mm]	d [mm]	t [mm]	B [mm]
1.	SP1/0.4	270,0	949	80,75	5,5	7,5	2,94	0,405	169,0
2.	SP2/0.4		950	79,30	6,0	8,5	5,68	0,404	167,1
3.	SP3/0.4		950	78,20	6,0	8,0	10,50	0,418	164,4
4.	SP4/0.4		950	79,75	6,0	8,5	12,54	0,419	168,0
5.	SP1/0.57	314,5	950	79,50	5,5	8,5	3,43	0,570	167,5
6.	SP2/0.57		950	80,15	6,0	8,2	5,21	0,569	168,5
7.	SP3/0.57		952	80,10	6,8	6,8	6,23	0,567	167,0
8.	SP4/0.57		950	80,50	6,5	7,0	9,30	0,567	168,0
9.	SP5/0.57		950	80,65	6,2	8,0	12,26	0,568	169,3
10.	SP1/0.63	270,0	948	78,25	5,5	9,5	3,10	0,634	166.0
11.	SP2/0.63		948	78,75	7,0	8,0	6,07	0,630	165,5
12.	SP3/0.63		948	79,30	7,0	7,0	9,10	0,635	165,6
13.	SP4/0.63		948	80,00	7,0	7,0	12,15	0,636	167,0
14.	SP5/0.63		948	78,35	6,5	11,5	23,50	0,630	168,0
15.	SP1/0.81	343,0	948	78,65	6,5	10,0	2,90	0,814	167,3
16.	SP2/0.81		948	78,70	7,0	7,0	5,92	0,796	164,4
17.	SP3/0.81		948	80,05	7,0	7,0	8,90	0,809	167,1
18.	SP4/0.81		948	81,50	7,0	7,0	11,50	0,838	170,0
19.	SP5/0.81		948	81,50	7,0	7,0	25,20	0,792	170,0
20.	SP1A/0.81	343,0	947	79,50	6,5	10,0	3,25	0,814	169,0
21.	SP2A/0.81		947	81,00	7,0	7,0	6,15	0,819	169,0
22.	SP3A/0.81		948	80,50	7,0	7,0	9,67	0,818	168,0
23.	SP4A/0.81		948	81,25	7,0	7,0	12,67	0,800	169,5
24.	SP5A/0.81		948	81,85	7,5	7,6	25,63	0,778	171,3
25.	SP6A/0.81		949	82,60	7,5	7,5	25,30	0,815	172,7
26.	SP1/1.2	262,0	948	78,75	6,5	10,0	5,23	1,170	167,5
27.	SP2/1.2		948	78,85	7,0	7,0	8,92	1,170	164,7
28.	SP3/1.2		948	80,75	7,5	7,5	9,47	1,198	169,0
29.	SP4/1.2		948	81,25	7,5	7,5	12,58	1,198	170,0
30.	SP5/1.2		948	81,50	7,5	7,5	25,25	1,198	170,5
31.	SP1/1.6	181,5	948	81,10	7,5	7,5	4,35	1,585	169,7
32.	SP2/1.6		948	78,45	7,6	7,6	9,34	1,601	164,5
33.	SP3/1.6		948	78,95	7,6	7,6	11,80	1,608	165,5
34.	SP4/1.6		948	78,35	8,0	8,0	16,48	1,603	164,7
35.	SP5/1.6		947	82,05	7,9	7,9	25,00	1,600	172,0

Table 2.

Comparison of the ultimate load of the plates according to different methods

No.	Spec. no.	Test results $\bar{P}_E$ [8]	Theory results P_{UR}	Code BS5950 $\bar{P}_{EF}$ [3]	Winter's formula
		[N]	[N]	[N]	[N]
1.	SP1/0.4	3694	3077	—	4256
2.	SP2/0.4	4637	1703	—	5282
3.	SP3/0.4	6595	2017	3787	5995
4.	SP4/0.4	7850	2017	3767	6147
5.	SP1/0.57	12816	4927	—	10899
6.	SP2/0.57	7521	4415	—	10110
7.	SP3/0.57	9634	7480	—	11340
8.	SP4/0.57	9456	4708	6917	11717
9.	SP5/0.57	12327	4800	7015	9023
10.	SP1/0.63	8455	4817	—	11239
11.	SP2/0.63	10680	9138	—	11834
12.	SP3/0.63	13261	6727	9492	12988
13.	SP4/0.63	17222	6980	11621	13536
14.	SP5/0.63	20470	7609	13634	14982
15.	SP1/0.81	14182	7850	—	15032
16.	SP2/0.81	16243	14220	—	19141
17.	SP3/0.81	21360	13750	—	23393
18.	SP4/0.81	28035	15310	17622	25643
19.	SP5/0.81	35244	14620	23920	26306
20.	SP1A/0.81	14997	8517	—	15712
21.	SP2A/0.81	18957	15130	—	20182
22.	SP3A/0.81	22784	14230	16379	24066
23.	SP4A/0.81	28258	13560	18356	23820
24.	SP5A/0.81	31239	13940	22816	25653
25.	SP6A/0.81	37825	15650	20050	27746
26.	SP1/1.2	31150	22800	—	28824
27.	SP2/1.2	38493	34530	—	34888
28.	SP3/1.2	42275	37630	—	37291
29.	SP4/1.2	46814	44520	51414	53332
30.	SP5/1.2	56293	50300	56925	47954
31.	SP1/1.6	33375	34660	—	34149
32.	SP2/1.6	45835	—	47877	—
33.	SP3/1.6	53400	—	55266	—
34.	SP4/1.6	56960	—	57408	—
35.	SP5/1.6	70310	—	70915	—

In the case of the plates with stiffeners characterised by low flexural rigidity, the minimum values of the critical loads have been obtained for the local

distortional mode, whereas for stiffeners characterised by high rigidity — for the local antisymmetric mode [9], [19]. It follows from the intermediate stiffener rigidity. If the rigidity of the stiffener is too low, the plate is not reinforced enough, and a stability loss in the plate and in the intermediate stiffener occurs at significantly lower stresses.

In the analysis of the elastic post-buckling state, only approximated estimation of the load carrying capacity can be obtained on the basis of the simplified failure criterion.

At this point of the present work, the following criterion of the limit load carrying capacity P_u for stiffened plates is assumed: "plastic stresses are reached in the plate for the limit load higher than the critical load P_{cr}".

In order to determine maximum stresses occurring in the plate after its local buckling, owing to the fact that the investigated plates were compressed, only the cross-section areas have been reduced.

Figure 2 presents the ratios of the theoretical and experimental values of loads $P_{uR}/\overline{P}_E$, whereas Fig. 3 - the ratio of the theoretical and standard (obtained according to BS 5950 Part 5) values of $P_{uR}/\overline{P}_{EF}$ as a function of I_s/I_{adeq}.

Lower values of the load carrying capacities P_{UR} than the experimental values $\overline{P}_E$ [8] have been obtained for all the cases investigated. Only in one case, the value of the failure limit load was a little lower than the theoretical value (case 31). In four cases (32-35) the values of local critical stresses are higher than the yield limit, and the buckling for these cases occurs in the elasto-plastic range. Here an approach suggested in, e.g., papers [12], [14] can by adopted.

In paper [16], a very significant influence of local imperfections upon the post-buckling limit load, which has been neglected in the present study, has been shown.

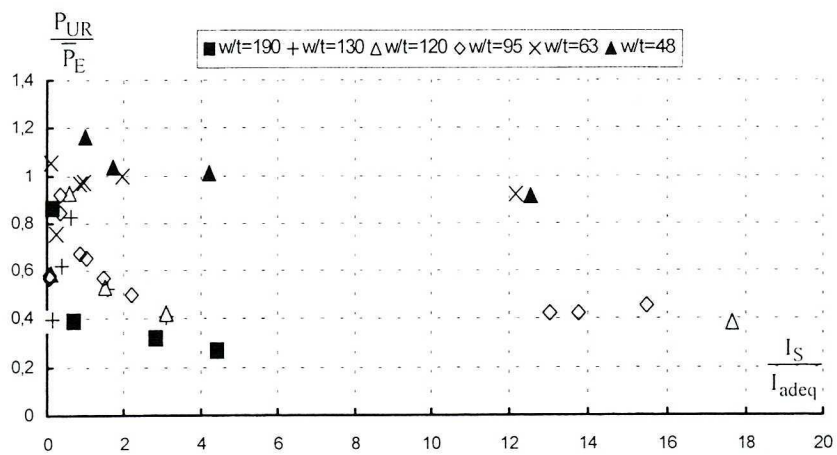

Fig. 2. Ratio of the theoretical and experimental values of $P_{UR} / \overline{P}_E$ as a function of I_S / I_{adeq}

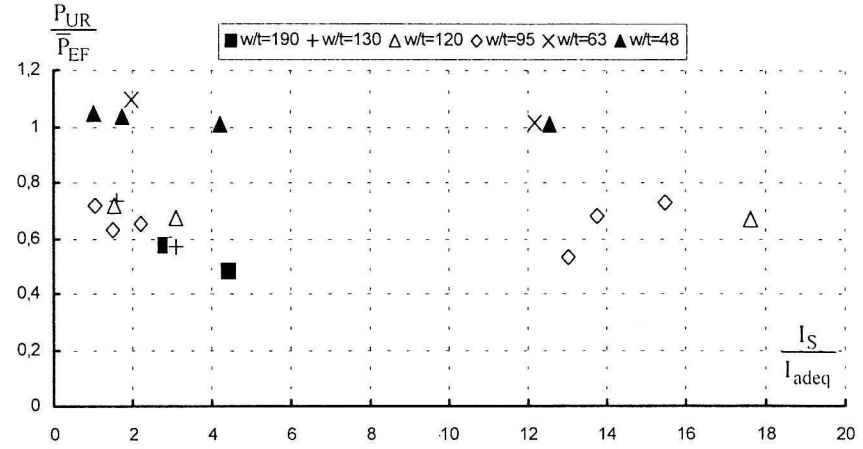

Fig. 3. Ratio of the theoretical and standard (obtained according to BS 5950 Part 5) values of $P_{UR} / \overline{P}_{EF}$ as a function of I_S / I_{adeq}

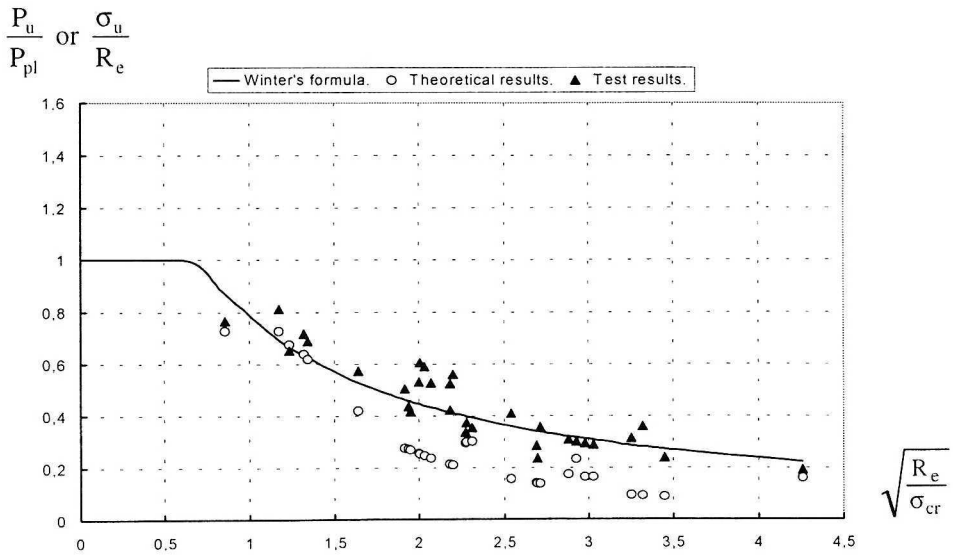

Fig. 4. Comparison of the ultimate load of the plates according to the Winter's rule

Local buckling modes corresponding to the lowest values of the critical loads predict correctly the type of failure mechanisms in stiffened plates under compression.

The nondimensionalized ultimate load (P_u/P_{pl}) or stress (σ_u/R_e) as a function of the dimensionless slenderness $\sqrt{R_e / \sigma_{cr}}$ has been plotted in Fig. 4. The experimental and theoretical values indicate a good agreement with the Winter's formula.

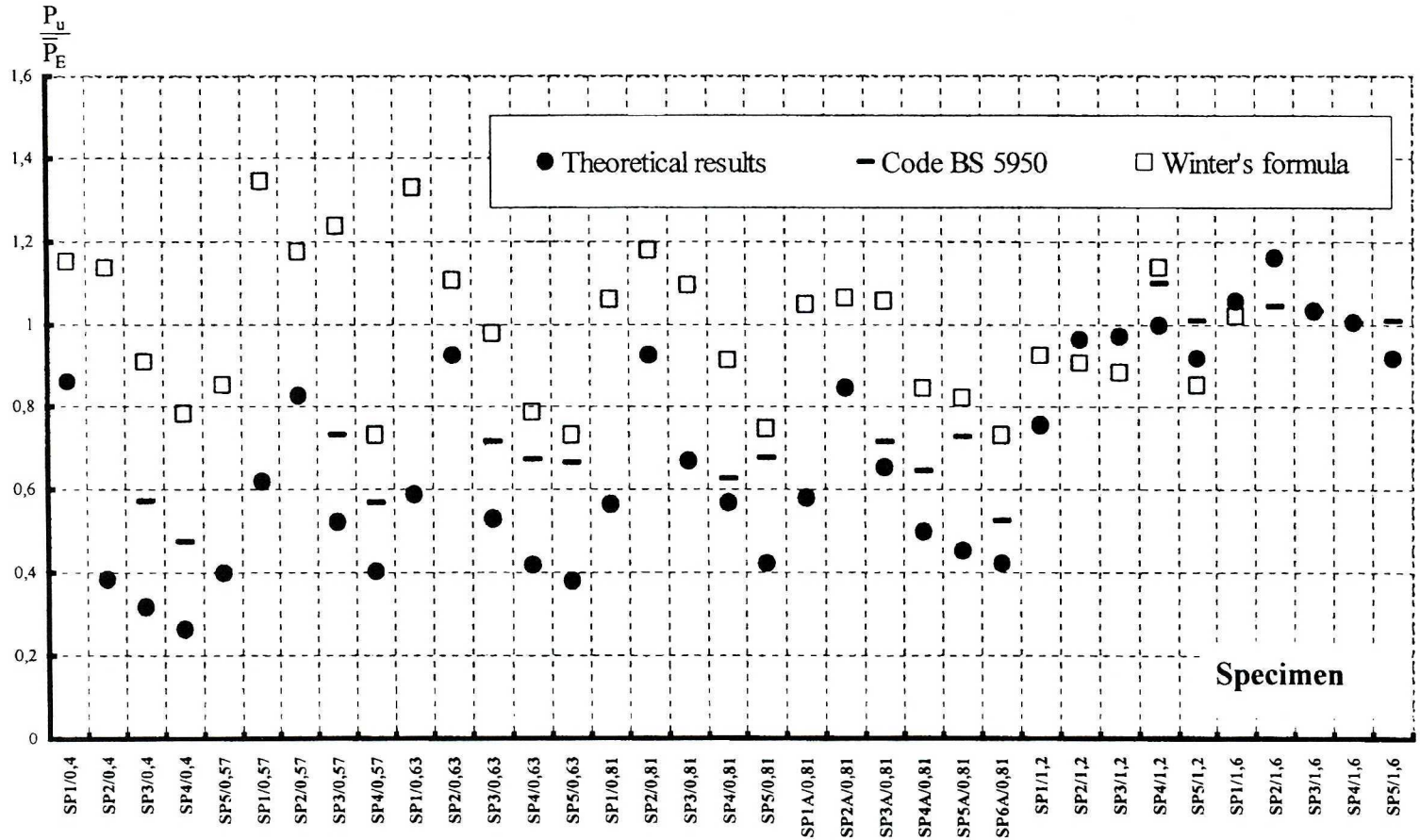

Fig. 5. Comparison of the ultimate load of the compressed plates according to different methods

4.2. Thin-walled beams with intermediate stiffeners

Next, the results of the presented theory have been compared with the experimental results obtained for beams with intermediate stiffeners under pure bending (Fig. 6a) [8]. Geometry of the cross-sections is shown in Fig. 6b and Table 3.

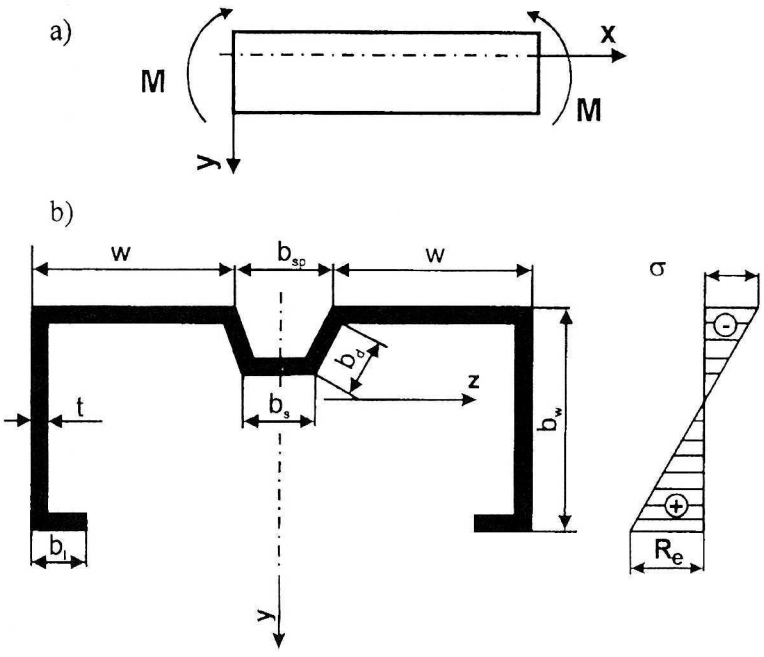

Fig. 6. Thin-walled beam under pure bending and cross-section of the beams with a central intermediate stiffener

A detailed comparison of the theoretical analysis results within the first order approximation and the experimental results has been included in [10].

At this point of the paper, the following criterion has been adopted for the load carrying capacity, M_E:

- in a plate under tension, the yield stress is attained at a limit load value higher than the critical moment M_{cr}. In a compressed plate, elastic strains are present;
- in a compressed plate, the yield stress is attained at a limit load value lower than the critical moment, M_{cr}. In this case we are dealing with the pre-buckling bending.

Such a criterion takes into account the post-buckling of plates under compression or a lack of this buckling in the pre-buckling state in perfect structures; it considers also a relevant mechanism of failure by means of yielding in the plate being compressed.

Table 3.

Dimensions of the channel beams with a central intermediate stiffener [8]

No.	Spec.	R_c [MPa]	L [mm]	w [mm]	b_s [mm]	b_{sp} [mm]	b_d [mm]	b_w [mm]	b_l [mm]	t [mm]
1.	LCO	214,5	1060	76,95	0,0	0,0	0,0	78,5	15,0	1,570
2.	A0			76,60	0,0	0,0	0,00	77,1	15,1	0,410
3.	A1			71,50	5,2	11,2	4,20	76,4	17,3	0,405
4.	A2	275.0	1060	73,10	6,5	8,1	5,56	77,4	17,5	0,410
5.	A3			73,55	6,6	7,1	9,00	76,8	16,6	0,410
6.	A4			73,65	6,8	7,2	11,80	76,9	18,0	0,415
7.	A5			73,35	6,6	8,0	18,20	76,9	17,1	0,405
8.	B1			70,55	4,7	13,2	6,00	76,9	17,6	0,682
9.	B2	374,0	1060	72,70	6,5	8,8	5,60	76,7	17,4	0,691
10.	B3			73,10	6,5	7,8	7,70	77,1	18,5	0,698
11.	B4			73,20	6,7	8,0	10,70	77,0	18,9	0,695
12.	C0			76,90	0,0	0,0	0,00	77,4	15,3	0,818
13.	C1			70,75	4,5	12,7	5,65	77,0	17,2	0,818
14.	C2	285,0	1060	72,65	5,7	9,5	5,45	76,7	17,7	0,821
15.	C3			73,85	6,9	7,3	8,70	77,4	17,1	0,814
16.	C4			73,60	7,0	7,4	11,70	77,0	18,5	0,815
17.	C5			73,35	6,9	7,6	18,20	77,5	18,2	0,810
18.	D1			71,25	5,5	9,5	4,55	76,5	16,2	0,759
19.	D2	147,4	1060	72,50	6,5	8,0	8,95	76,4	25,5	0,761
20.	D3			72,15	6,2	8,2	11,35	76,2	16,8	0,762
21.	D4			72,40	6,2	8,2	15,10	76,9	9,0	0,763
22.	E1			71,65	7,0	11,0	4,85	76,3	17,0	1,213
23.	E2			72,30	7,0	10,0	5,10	77,8	17,0	1,207
24.	E3	176,5	1060	73,55	7,0	7,0	8,20	79,0	18,0	1,207
25.	E4			73,20	7,0	8,1	9,00	77,2	14,5	1,200
26.	E5			73,80	7,7	7,7	12,00	76,7	17,0	1,209
27.	E6			73,50	7,5	7,5	18,80	78,7	17,5	1,202
28.	F1			70,25	5,2	13,0	5,10	76,0	17,7	1,519
29.	F2			70,90	5,5	12,0	6,00	75,5	17,8	1,528
30.	F3	214,5	1060	71,75	6,2	10,0	9,70	76,3	17,0	1,528
31.	F4			71,50	6,5	10,5	12,55	76,3	15,5	1,514
32.	F5			71,63	7,0	9,75	18,25	77,6	18,5	1,525

However, in order to determine maximum stresses in the plate after the local buckling of the beam, one must find not only the reduced flexural stiffness but also the position of the effective stiffness centre of the cross-section.

The above-mentioned thin-walled beams are considered as calculation examples. Generally speaking, one has to find the effective width of a plate under compression and of webs subject to bending. In this paper, only the width

of a compressed flange is reduced so as to obtain an actual decrease in flexural stiffness of the cross-section after buckling. The effective width of the compressed plate is derived from the condition saying that the moment of inertia of the effective cross-section corresponds to the expression for the coefficient of reduced flexural stiffness, η (6).

Table. 4.
Comparison of the ultimate moment of the channel beams according to different method

No.	Spec. no.	Test results $\bar{M}_E$ [8] [Nm]	Theory results M_E [Nm]	Code BS5950 $\bar{M}_{EF}$ [3] [Nm]	Code PN-90/B-03200 [Nm]	Winter's formula [Nm]
1.	LCO	3223,1	2257	—	1699,0	2716,4
2.	A0	339,0	575,1	—	522,0	335,1
3.	A1	350,8	468,0	—	546,6	336,2
4.	A2	375,7	612,5	—	571,8	435,6
5.	A3	349,6	591,4	502,7	554,5	424,2
6.	A4	318,9	619,6	464,7	582,5	444,6
7.	A5	306,4	587,6	440,7	553,5	521,0
8.	B1	1177,8	1126,9	—	1298,4	1255,7
9.	B2	1250,0	1286,8	—	1310,6	1331,0
10.	B3	1291,4	1443,0	—	1376,0	1377,7
11.	B4	1273,3	1444,9	1372,7	1378,6	1374,6
12.	C0	1232,7	1202,8	—	1147,0	815,2
13.	C1	1395,0	1021,8	—	1211,5	1323,6
14.	C2	1489,6	1229,7	—	1229,7	1164,5
15.	C3	1463,0	1308,5	1373,9	1308,5	1687,2
16.	C4	1380,2	1328,9	1262,5	1328,9	1543,1
17.	C5	1377,2	1311,3	1245,7	1311,3	1517,6
18.	D1	889,2	840,8	—	840,8	986,3
19.	D2	1023,4	1044,7	1253,6	1044,7	934,8
20.	D3	924,2	913,5	1096,2	913,5	858,1
21.	D4	877,3	810,8	1013,5	810,8	767,7
22.	E1	1909,0	1755,6	—	1755,6	1749,4
23.	E2	1904,9	1802,9	—	1802,9	1802,9
24.	E3	2045,1	1877,5	2065,3	1877,5	1877,5
25.	E4	1930,8	1698,3	1953,1	1698,3	1698,3
26.	E5	1980,8	1765,7	2030,6	1765,7	1765,7
27.	E6	1980,8	1836,7	2020,4	1836,7	1836,7
28.	F1	2712,1	2673,4	—	2673,4	2617,0
29.	F2	2918,3	2671,6	—	2671,6	2671,6
30.	F3	2924,2	2679,7	—	2679,7	2679,7
31.	F4	2687,6	2585,2	2714,5	2585,2	2585,2
32.	F5	2829,5	2797,8	2937,7	2797,8	2797,8

The plate model that has been assumed in the calculations allows one to take into account an influence of global imperfections on the values of reduced local critical loads of the beams under compression, which is impossible in the case the beam model is assumed. In papers [10], [16], a method for lower bound estimation of the load carrying capacity has been discussed in detail. In [10], higher values were obtained for the theoretical limit load carrying capacity than for the experimental limit load carrying capacity. Hence, the second order approximation provides a better estimation of the load carrying capacity of beams under bending.

Table 4 includes a comparison of the results M_E and the experimental $\bar{M}_E$ [8] values of the limit loads to the results calculated in three other manners. The codes used were the Polish Code PN-90/B-03200 [18], the British Code BS 5950 Part 5 [3] and the method based on the Winter's formula. In all the analysed cases, a good agreement is found between the presented lower bound estimation of the load carrying capacity M_E and the experimental results $\bar{M}_E$.

Figures 7 and 8 show the ratios of the theoretical and experimental values of loads $M_E / \bar{M}_E$ and the ratio of the theoretical and standard (obtained according to BS 5950, Part 5) values of $M_E / \bar{M}_{EF}$ as a function of I_s/I_{adeq}.

The nondimensionalized ultimate moments (M_u/M_{pl}) or stresses (σ_u/R_e) as a function of the dimensionless slenderness $\sqrt{R_e / \sigma_{cr}}$ have been plotted in Fig. 9. The experimental and theoretical values indicate a good agreement with the Winter's formula. Figure 9 shows that the correlation of all the results becomes better when the dimensionless slenderness becomes smaller. For higher dimensionless slenderness, the theory and test results do not agree so well with the Winter's formula, although the agreement is still fair.

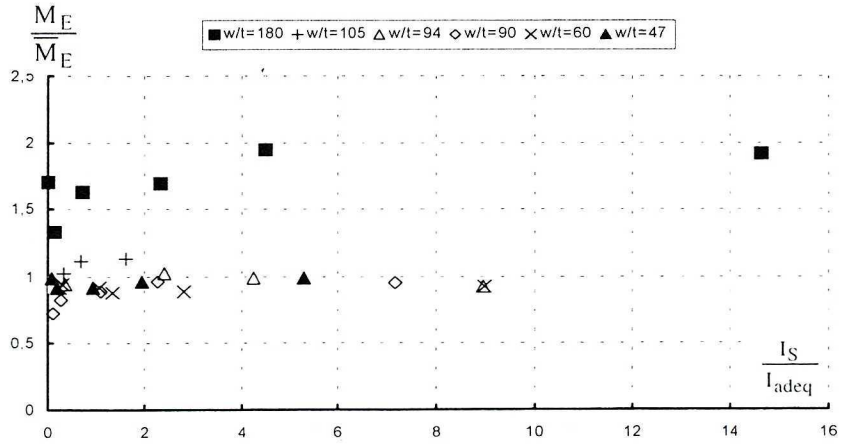

Fig. 7. Ratio of the theoretical and experimental values of $M_E / \bar{M}_E$ as a function of I_S / I_{adeq}

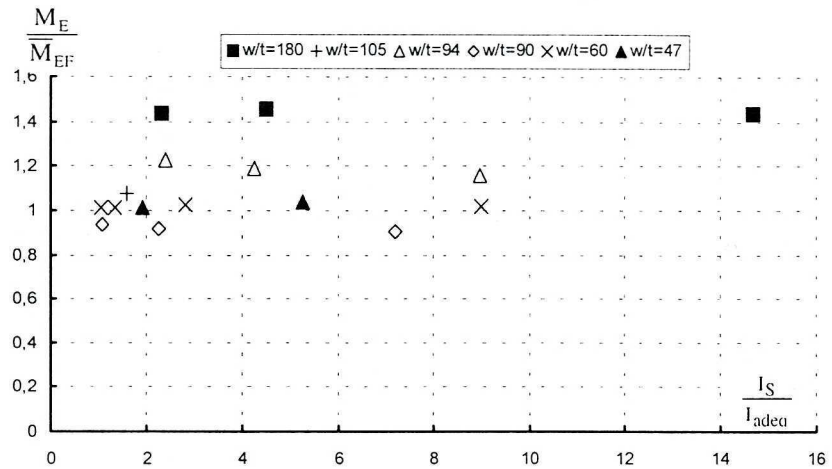

Fig. 8. Ratio of the theoretical and standard (obtained according to BS 5950 Part 5) values of $M_E / \bar{M}_{EF}$ as a function of I_S / I_{adeq}

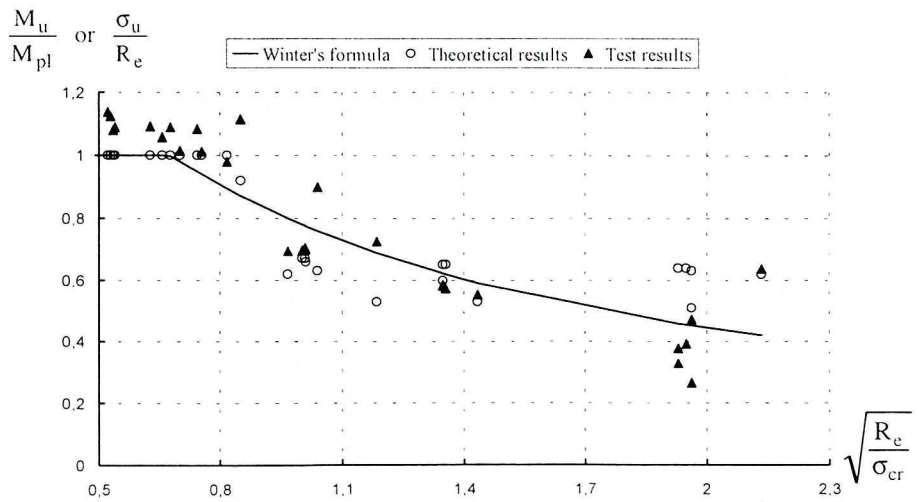

Fig. 9. Comparison of the ultimate moment of the channel beams according to the Winter's rule

Figure 10 shows the comparisons between the theoretical ultimate moment and those determined using the British Code BS 5950 Part 5, the Polish Code PN-90/B-00320 and the method based on the Winter's formula, respectively. Figure 10 indicates that for the channel beams, the test results are in a fairly reasonable agreement with the ultimate moment predictions of all three codes. All specifications are similar in their approach to calculating the ultimate moment capacity. The main differences between the specification results arise from the application of the imperfection factor and the modulus of elasticity values used in the calculations.

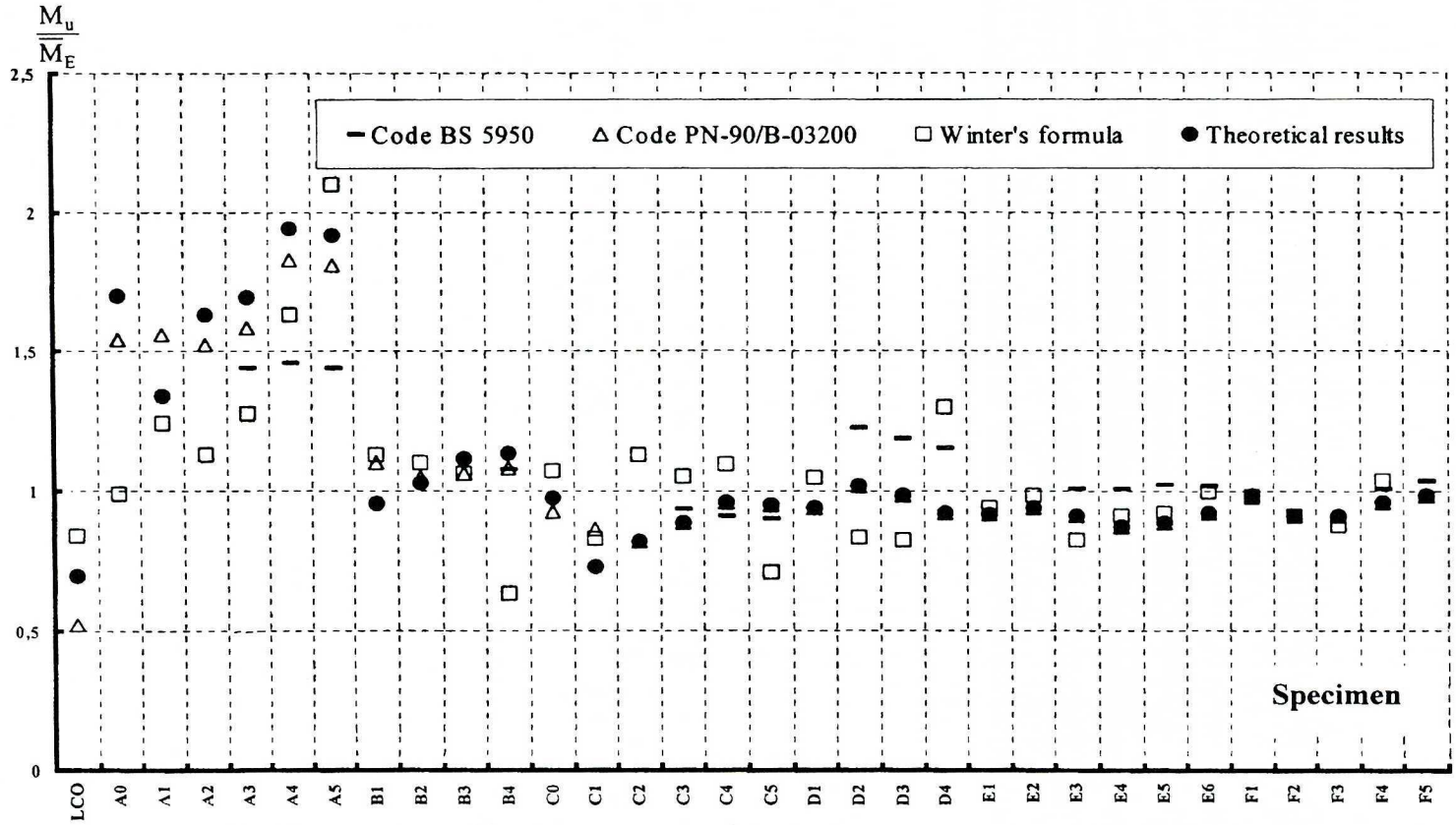

Fig. 10. Comparison of the ultimate moment of the channel beams according to different methods

5. Conclusions

The interactive buckling analysis of thin-walled structures with an intermediate stiffener under axial compression or/and a constant bending moment, carried out by means of the transition matrix method, has been presented. All global and local modes are described by means of the plate theory. The presented analysis provides correct lower bound estimation of the load carrying capacity of thin-walled structures with intermediate stiffeners under compression or bending and it predicts correctly failure mechanisms, which is impossible if the beam model is assumed. A good agreement of the theory presented here with the results of investigations carried out by other authors and with numerous cases of standards in force has been obtained. The next publication by the authors that is now being prepared to be printed, will be devoted to significant differences occurring in some cases between the results of the presented theory and standards. A comparison of the results obtained when the effect of global bending on local buckling is taken into account allows one to state that lower bound estimation of the load carrying capacity of beams under bending produces lower values than those obtained for one-mode buckling [10]. In [10] higher values of the theoretical load carrying capacity than of the experimental ones have been obtained. Thus, the method being proposed gives, in this case, more correct evaluation of the load carrying capacity for the thin-walled structures under analysis. The presented method of calculations allows for taking into account an effect of local pre-buckling and an influence of local initial imperfections on the coefficient of reduced rigidity [16].

In the case the global stresses exceed the minimum local stress, it is possible to attain the load carrying capacity higher than the minimum local stress value for sufficiently small imperfections.

Intermediate stiffeners are found to exert a strong influence on local buckling modes.

Manuscript received by Editorial Board, October 24, 2000;
final version, December 05, 2000.

REFERENCES

[1] AISI. Specification for the Design of Cold-formed Steel Structural Members. American Iron and Steel Institute, Washington, D.C., 1989.

[2] Biderman B.L.: Mechanics of thin-walled structures – Statics. Moscow, Mashinostroenie, 1977, pp. 488 (in Russian).

[3] BS 5950. Structural Use of Steelwork in Building — Part 5: Code of Practice for the Design of Cold Formed Sections. London 1990.

[4] Byskov E., Hutchinson J.W.: Mode interaction in axially stiffened cylindrical shells. AIAA J., 15, 7, 1977, pp. 941÷948.

[5] Camotim D., Prola I.C.: On the stability of thin-walled columns with Z, S and sigma sections. Proc. of Second Int. Conf. on Coupled Instability in Metal Structures, Imperial Press College, 1996, pp.149÷156.

[6] Cold-formed steel structures, Standards Assoc. of Australia, N.S.W., Australia, 1988.

[7] Dubina D.: Coupled instabilities in bar members – general report. Proc. of Second Int. Conf. on Coupled Instability in Metal Structures, Imperial Press College, 1996, pp.119÷132.

[8] Hoon K.H., Rhodes J., Seah L.K.: Tests on intermediately stiffened plate elements and beam compression elements. Thin-Walled Structures, 16, 1993, pp.111÷143.

[9] Kolakowski Z., Teter A.: Interactive buckling of thin-walled closed elastic column-beams with intermediate stiffeners. Int. J. Solids Structures, Vol.32, No.11, 1995, pp.1501÷1516.

[10] Kolakowski Z., Teter A.: Influence of local post-buckling behaviour on bending of thin-walled elastic beams with central intermediate stiffeners. Engineering Transactions, 43, 3, 1995, pp.383÷396.

[11] Kolakowski Z., Teter A.: Interactive buckling of thin-walled beam-columns with intermediate stiffeners or/and variable thickness. Int. J. Solids Structures Vol. 37, No 24, 2000, pp. 3323÷3344.

[12] Kolakowski Z., Kowal-Michalska K., Kedziora S.: Determination of inelastic stability of thin-walled isotropic columns using elastic orthotropic plate equations. Mechanics and Mechanical Engineering, Vol. 1, No. 1, 1997, pp.79÷100.

[13] Kolakowski Z., Kowal-Michalska K. (ed.): Selected problems of instabilities in composite structures. Series of monographies. Technical University of Lodz, 1999.

[14] Kowal-Michalska K., Kolakowski Z., Kedziora S.: Global and local inelastic buckling of thin-walled orthotropic columns by elastic asymptotic solutions. Mechanics and Mechanical Engineering, 2, 2, 1998, pp. 209÷232.

[15] Krolak M. (ed.): Post-buckling behaviour and load carrying capacity of thin-walled plate girders. PWN, Warsaw-Lodz, 1990, p. 553.

[16] Manevich A. I., Kolakowski Z.: Influence of local postbuckling behaviour on bending of thin-walled beams. Thin-Walled Structures, Vol. 25. No 3, 1996, pp.219÷230

[17] Manevich A.I., Kolakowski Z.: Multiple interaction of buckling modes and imperfection sensitivity in compressed thin-walled members. Conference of GAMM, Regensburg, 1997.

[18] PN-90/B-03200 Konstrukcje stalowe. Obliczenia statyczne i projektowanie. Wydawnictwo Normalizacyjne, Warszawa 1994.

[19] Teter A., Kolakowski Z.: Interactive buckling of thin-walled open elastic beam-columns with intermediate stiffeners. Int. J. Solids Structures, Vol.33, No.3, 1996, pp.315÷330.

Porównanie teoretycznych i eksperymentalnych obciążeń granicznych dla wybranych dźwigarów i płyt cienkościennych z żebrami

Streszczenie

W prezentowanej pracy wyznaczono teoretyczne wartości nośności granicznej dla cienkościennych dźwigarów i płyt z centralnymi, wzdłużnymi żebrami pośrednimi obciążonych osiową siłą ściskającą i stałym momentem gnącym. Nieliniowe zagadnienie stateczności rozwiązano stosując teorię Byskova i Hutchinsona [4] wykorzystując w obliczeniach numeryczną metodę macierzy przejścia. W prezentowanej metodzie oszacowania współczynników redukcji

sztywności wzdłużnej postuluje się wyznaczenie zredukowanego lokalnego obciążenia krytycznego z uwzględnieniem globalnego dokrytycznego zginania w ramach pierwszego nieliniowego rzędu przybliżenia teorii interakcyjnego wyboczenia konstrukcji. Otrzymane wyniki porównano z wynikami opublikowanymi przez innych autorów oraz z wartościami obliczonymi wg obowiązujących norm.